© S. Hirzel Verlag
Stuttgart

Experimental Study of Gas Bubble Oscillations Using a Shock Tube

K. Vokurka, A. E. Beylich, H. Kleine
Stoßwellenlabor, Technische Hochschule Aachen

Experimental Study of Gas Bubble Oscillations Using a Shock Tube

Summary

Free oscillations of gas bubbles in a liquid are studied in detail. A shock tube is used to generate the pressure step in the liquid necessary to excite the bubble for free oscillations. Bubble wall motion is recorded using a rotating mirror camera and acoustic waves radiated by the bubble are monitored using a needle hydrophone. By varying the step size of the driving pressure different bubble oscillation intensities are investigated. The experimental data obtained are compared with theoretical predictions and, generally, a relatively good agreement between theory and experiment is found. However, a few interesting deviations are also observed and discussed.

Experimentelle Untersuchung von Gasblasenoszillationen in einem Stoßrohr

Zusammenfassung

Freie Gasblasenoszillationen in einer Flüssigkeit werden detailliert untersucht. Der zur Schwingungsanregung benötigte Drucksprung in der Flüssigkeit wird mit Hilfe eines Stoßrohres erzeugt. Die Bewegung der Blasenwand wird mittels einer Hochgeschwindigkeits-Drehspiegelkamera aufgezeichnet; zur Messung der von der Blase ausgestrahlten akustischen Wellen wird ein Nadelhydrophon verwendet. Die Variation des Drucksprungs erlaubt die Untersuchung verschiedener Schwingungsintensitäten. Die experimentellen Daten werden mit theoretischen Berechnungen verglichen, wobei sich generell eine recht gute Übereinstimmung zwischen Theorie und Experiment ergibt. Einige interessante Abweichungen werden allerdings auch beobachtet und diskutiert.

Etude expérimentale des oscillations de bulles gazeuses à l'aide d'un tube à onde de choc

Sommaire

Nous avons étudié en détail les oscillations libres de bulles gazeuses en milieu liquide. L'échelon de pression nécessaire pour exciter les oscillations libres des bulles a été produit dans un tube à onde de choc. On a enregistré le mouvement des parois des bulles à l'aide d'une caméra à miroir tournant, et capté les ondes rayonnées au moyen d'un hydrophone aiguille. En faisant varier l'ampleur de la surpression excitatrice, il a été possible d'examiner différentes amplitudes d'oscillation des bulles. La comparaison des résultats expérimentaux et des prévisions théoriques fait apparaître un accord relativement bon. Il y a cependant quelques écarts remarquables, que l'on discute, entre théorie et expérience.

1. Introduction

Oscillations of bubbles in liquids represent an intriguing physical problem that has been intensively studied for several decades. Recent work has concentrated on bubble oscillations near boundaries [1], regular and chaotic bubble oscillations [2], thermodynamics of vapour bubbles [3], multiscale analysis of bubble oscillations [4, 5], and investigations of laser-induced bubble oscillations [6, 7]. Experimental techniques include, for example, time-resolved particle image velocimetry [8], and interferometric studies [9].

In spite of great efforts there are still several points not fully understood. For example, excessive energy losses from oscillating bubbles have been reported [10, 11]. However, the corresponding dissipation mechanism has not been identified yet. This problem of unknown energy losses has motivated us to perform a detailed experimental study of both the bubble wall motion and of radiated acoustic waves with the aim of obtaining a more complete picture of the bubble behaviour. The bubbles were excited into free oscillations by a pressure step generated in a shock tube. A similar technique has been successfully used in previous works [12–14]. The bubble wall motion was recorded by a rotating mirror camera, and the pressure waves radiated by the bubble were monitored with a needle hydrophone. By varying the gas pressure in the shock tube, pressure steps of different intensities could be generated in the liquid. This made it possible to study the bubble oscillations under a variety of conditions. However, because the bubble usually lost its initial spherical shape at later times, only the first compression and expansion phases were investigated.

Received 21 June 1991,
accepted 30 August 1991.

K. Vokurka, Švédská 27, Jablonec n.N., CS-46602, ČSFR.

A. E. Beylich, H. Kleine, Stoßwellenlabor, Technische Hochschule Aachen, D-5100 Aachen, Germany.

The measured experimental data allow for a comparison with theoretical results obtained by integrating the equation of motion for the bubble wall and by subsequently computing the radiated acoustic wave.

2. A gas bubble model

Let us consider a spherical gas bubble of an initial radius R_i occurring in a viscous compressible liquid, and let the initial ambient pressure in the liquid be $p_{\infty i}$. At a time $t = 0$ the pressure in the liquid increases linearly up to a new value $p'_\infty = p_{\infty i} + \Delta p$ where it remains constant for a time ΔT; here ΔT is much larger than the rise time Δt of the pressure step Δp, i.e. $\Delta T \gg \Delta t$. The assumed variation of the ambient pressure p_∞ with time is shown in Fig. 1.

Due to the ambient pressure change the bubble-liquid system leaves its equilibrium state, and the bubble starts to oscillate. Initially, the bubble is compressed to a minimum radius R_{m1} with the compression phase lasting for a time T_{c1}. At the minimum volume the bubble wall motion reverses and, during the subsequent expansion phase, the bubble grows to a maximum radius R_{M2}. Note that due to energy losses $R_{M2} < R_i$. During the life of the bubble compression and expansion phases occur several times. Due to the bubble volume changes the pressure in the gas inside the bubble also varies and an outward travelling spherical acoustic wave p_a is radiated.

In this study only relatively small pressure steps Δp will be considered. This means that the bubble oscillations are moderate as well. To describe a bubble wall motion under these circumstances a simplified Herring's model can be used, where the simplification consists in the omission of the correcting terms. In this case the equation of motion for the bubble wall can be written as [15]

$$\ddot{R}R + \frac{3}{2}\dot{R}^2 = \frac{1}{\varrho_\infty}(P - p_\infty + \dot{P}R/c_\infty). \tag{1}$$

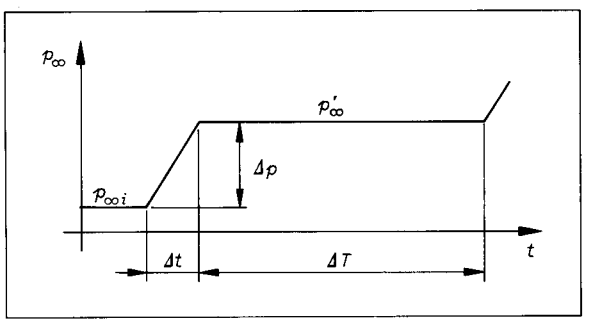

Fig. 1. Variation of the ambient pressure p_∞ with time t.

Here R denotes the bubble radius, ϱ_∞ the liquid density, P the pressure in the liquid at the bubble wall, p_∞ the time dependent ambient pressure (see Fig. 1) and c_∞ the speed of sound in the liquid. Dots denote differentiation with respect to time. The initial conditions of eq. (1) are $R(0) = R_i$ and $\dot{R}(0) = 0$. The accuracy of eq. (1) was carefully checked against the original Herring's equation and the difference was found to be negligible.

For sufficiently large bubbles the gas inside the bubble may be assumed to behave adiabatically. Then the pressure in the liquid at the bubble wall can be written as

$$P = (p_{\infty i} + 2\sigma/R_i)(R/R_i)^{-3\gamma} - 2\sigma/R - 4\eta\dot{R}/R, \tag{2}$$

where γ is the ratio of the specific heats, σ the surface tension and η the dynamic viscosity of the liquid.

For moderate bubble oscillation intensities the acoustic wave p_a radiated by the bubble can be conveniently determined using a simple expression

$$p_a = p - p_\infty = (P - p_\infty + \tfrac{1}{2}\varrho_\infty \dot{R}^2)\, R/r. \tag{3}$$

Here p is the total pressure field in the liquid and r is the point in the liquid in which p_a is being determined. Note that the total pressure field p is given by superposition of the driving ambient pressure field p_∞ and the radiated acoustic wave p_a. Let us also note that eq. (3) is valid for $r > R_i$ only.

The acoustic energy ΔE_a radiated by the bubble during a time interval (t_1, t_2) can be determined using the formula

$$\Delta E_a = 4\pi r^2 \frac{1}{\varrho_\infty c_\infty} \int_{t_1}^{t_2} p_a^2 \, dt. \tag{4}$$

The radiated acoustic wave consists of a train of several pressure pulses called bubble pulses. To describe the bubble pulses in the time domain an effective pulse width ϑ can be defined by the relation

$$\vartheta = \frac{1}{p_p^2} \int_{t_1}^{t_2} p_a^2 \, dt, \tag{5}$$

where p_p is the peak pressure in the bubble pulse and t_1, t_2 are usually identified with the time instants of two consecutive pressure minima.

The total energy losses from the bubble can be characterized by a damping factor α defined as the quotient of two consecutive maximum radii, i.e.

$$\alpha_1 = R_{M2}/R_i. \tag{6}$$

Eqs. (1) to (6) can easily be solved numerically. With respect to the experiments reported later the computations have been performed for nitrogen bubbles oscillating in 85% diluted glycerine with the initial ambient pressure $p_{\infty i}$ being equal to atmospheric pressure.

In this case the values of the physical constants used are:

$p_{\infty i} = 100\,\text{kPa}$, $\varrho_\infty = 1220\,\text{kg m}^{-3}$, $c_\infty = 1920\,\text{ms}^{-1}$, $\sigma = 0.066\,\text{N m}^{-1}$, $\eta = 0.062\,\text{kg s}^{-1}\,\text{m}^{-1}$, $\gamma = 1.4$.

Computations were performed for bubbles with initial radii $R_i = 1.65$ mm (an exception is Fig. 2, where $R_i = 1.67$ mm) and for pressure steps having a rise time $\Delta t = 20$ μs. Let us note that for bubbles of this size the surface tension plays a negligible role, and viscosity only a minor one.

An example of a computed bubble wall motion is given in Fig. 2 while Fig. 3 presents the computed radiated acoustic wave. The values of the pressure steps Δp, initial radii R_i, and the point in the liquid r were selected in such a way as to allow for comparison with experimental records given in the following section (Figs. 5 and 7). In Fig. 3, T_{c1} denotes the compression time, T_{o2} the oscillation period, p_{p1} and p_{t2} the peak and trough pressures, respectively.

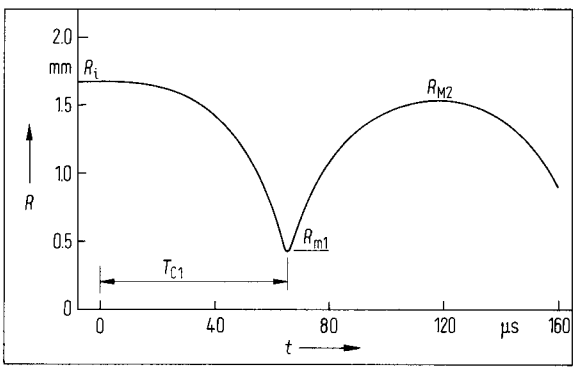

Fig. 2. Computed variation of the radius R with time t for a nitrogen bubble oscillating in glycerine under the action of a pressure step $\Delta p = 1.06$ MPa. Initial bubble radius $R_i = 1.67$ mm.

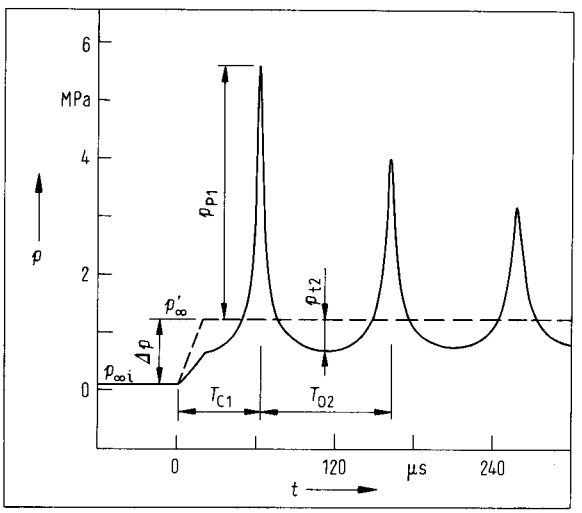

Fig. 3. Computed variation of the pressure p in the liquid with time t at a distance $r = 3$ mm from the centre of a nitrogen bubble oscillating in glycerine. Initial bubble radius $R_i = 1.65$ mm, the pressure step $\Delta p = 1.125$ MPa.

To describe the intensity of the bubble oscillations it is convenient to introduce the amplitude A, which is defined as the quotient of the maximum and the equilibrium radius, i.e.

$$A = R_M/R_e. \tag{7}$$

Here R_e is the equilibrium radius under the pressure p'_∞. In the case of the first compression phase it holds that $R_M = R_i$ and hence $A_1 = R_i/R_e$. It can be shown that for infinitely steep pressure steps ($\Delta t = 0$) the following equation is valid [11]:

$$A_1 = (p_{\infty i}/p'_\infty)^{-1/3\gamma}, \tag{8}$$

which can be further rearranged ($p'_\infty = p_{\infty i} + \Delta p$) to give:

$$A_1 = (1 + \Delta p/p_{\infty i})^{1/3\gamma}. \tag{9}$$

As has been mentioned, eq. (9) holds exactly for the case $\Delta t = 0$ only. However, it was verified numerically that eq. (9) can be used with sufficient accuracy even for the N_2 bubble in glycerine for $R_i = 1.65$ mm, $\Delta t = 20$ μs and $\Delta p < 15\,p_{\infty i}$.

3. Experimental arrangement

The experimental arrangement used for gas bubble dynamics studies is schematically shown in Fig. 4. A vertical shock tube (total length 4370 mm) consisted of three sections: the high-pressure section was filled with a driver gas (nitrogen) at a pressure p_4. The low-pressure section contained air at atmospheric pressure $p_1 = 0.1$ MPa. The lowest section of the tube was filled with 85% diluted glycerine. Glycerine was used because of its higher viscosity which made it possible for rising bubbles to retain a spherical shape. The high- and low-pressure sections were separated by a hostaphan membrane. Underneath the membrane two heating wires were stretched. When a condenser battery was discharged across the wires the stressed membrane melted along the contact lines with the wires and was torn up, thus initiating a shock wave.

The experimental nitrogen bubbles were generated with a small L-shaped tube submerged in the liquid. The nitrogen was supplied to the L-tube via a needle valve. By careful setting of the valve, a steady train of gas bubbles could be generated with a time interval between two consecutive bubbles ranging from 3 to

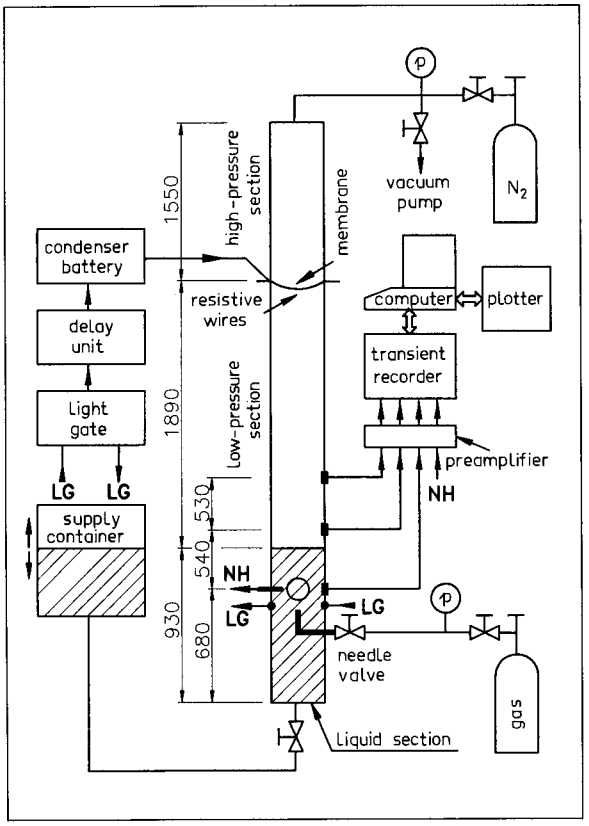

Fig. 4. Experimental apparatus for bubble dynamics studies (NH – needle hydrophone, LG – light gate).

5 s. The generated bubbles rose with a velocity of about 0.06 ms^{-1}. When the rising bubble interrupted the beam of a light gate, a trigger pulse was sent off and, after a preset delay, the condenser battery was discharged. Following that, the membrane was torn up and a shock wave propagating downwards was formed in the low-pressure section. At the liquid surface the shock wave was partially reflected and partially transmitted into the glycerine. The transmitted pressure step had approximately the form shown in Fig. 1 with $\Delta t \approx 20$ μs [16]. The pressure step strength Δp varied according to p_4; for maximum allowable pressure $p_4 = 2.4$ MPa it was approximately $\Delta p \approx 1.1$ MPa.

In the liquid the wave continued propagating downwards. After reflection at the bottom it was several times successively reflected at the liquid surface and at the bottom before being completely attenuated. For experiments with bubbles only the first, almost constant, part of the pressure step lasting ΔT could be used. For glycerine and the experimental arrangement shown in Fig. 4 this time interval was approximately $\Delta T \approx 750$ μs [16].

The pressure in the gas and in the liquid were monitored both by pressure transducers (PCB type 113A24) mounted flush with the shock tube wall and by a needle hydrophone (Imotec, Germany). The needle hydrophone was inserted into the liquid through a holder in the shock tube wall and its sensitive area was usually set at a distance $r = 3$ mm from the centre of the bubble. The signals from the pressure transducers and needle hydrophone were recorded by a transient recorder (Rene Maurer type TM 509) with a sampling interval usually set at 0.6 μs and with an amplitude discrimination of 8 bits. The recorded signals were further stored on a floppy disk and later processed by a personal computer. The value of the pressure step Δp was determined from the reflected shock wave using pressure records obtained by a transducer situated immediately above the liquid surface. Further details on the experimental arrangement can be found in [16].

An example of a recorded acoustic wave radiated by an oscillating bubble is shown in Fig. 5. Here a precursor occurring at the foot of the first bubble pulse leading edge was used as the zero time mark.

The bubble wall motion was studied by a rotating mirror camera with framing rates up to $2.5 \cdot 10^5\ s^{-1}$. A sketch of the optical apparatus is given in Fig. 6. A ruby laser (JK-Laser, system 2000, wavelength $\lambda = 694$ nm) was used as a source of a train of light pulses of approximate duration $10 \cdots 12$ ns each. The laser was triggered by the pressure transducer in the gas. A maximum of 310 frames could be obtained during one experiment which was sufficient to cover several oscillation periods. Again, the precursor, which could be seen on some frames (unfortunately not always), was used as the zero time mark. An example of the photographs obtained this way is shown in

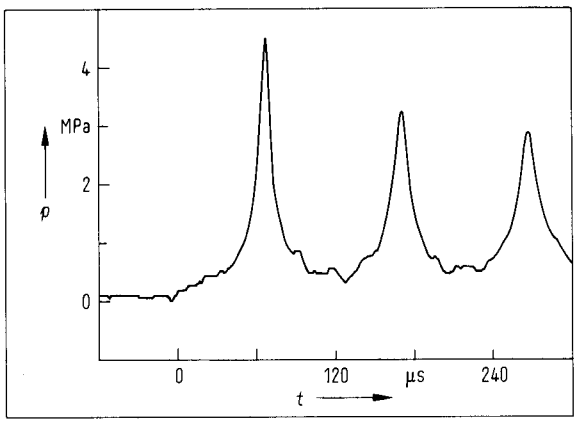

Fig. 5. A pressure wave radiated by a nitrogen bubble oscillating in glycerine. The wave was measured at a distance $r = 3$ mm from the bubble centre. Initial bubble radius $R_i = 1.65$ mm, the pressure step $\Delta p = 1.125$ MPa.

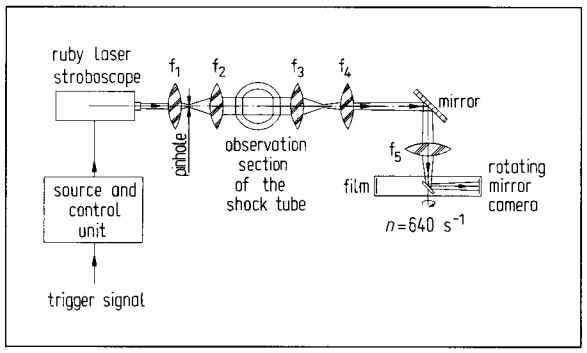

Fig. 6. Experimental apparatus for photographing the bubble oscillations using a rotating mirror camera. Focal lengths: $f_1 = 30$ mm, $f_2 = f_3 = 300$ mm, $f_4 = 120$ mm, $f_5 = 500$ mm.

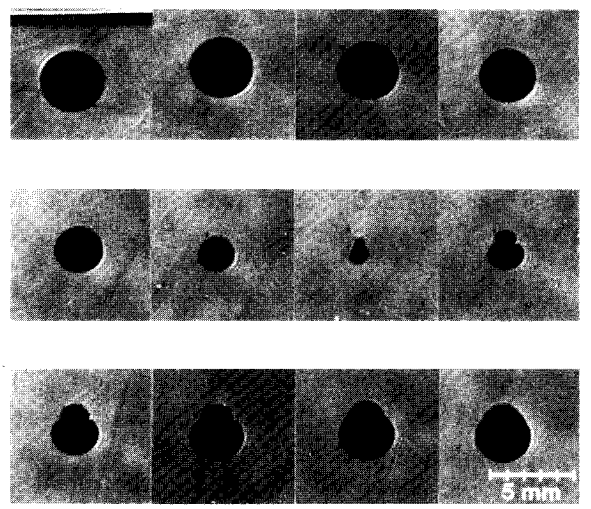

Fig. 7. A nitrogen bubble oscillating in glycerine. Time interval between frames 12 μs, initial bubble radius $R_i = 1.67$ mm, the pressure step $\Delta p = 1.06$ MPa.

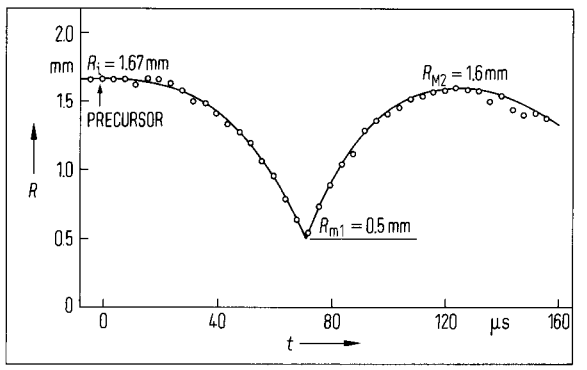

Fig. 8. Experimentally determined variation of the bubble radius R with time t for a nitrogen bubble oscillating in glycerine. Initial bubble radius $R_i = 1.67$ mm, the pressure step $\Delta p = 1.06$ Mpa.

Fig. 7. In this case the highest framing rate $2.5 \cdot 10^5\ s^{-1}$ was used, i.e. the time interval between subsequent frames was 4 μs. However, only every third frame is displayed in Fig. 7 and the selected frames are limited to the first compression and expansion phases. The precursor can be seen in the first frame. Note also that during the expansion phase the initially spherical shape of the bubble was distorted. The deformation is symmetrical with respect to the direction of the pressure step propagation with its extent growing with Δp. For low Δp (approximately for $\Delta p < 0.5$ MPa) the bubble preserves its spherical shape during the whole experiment. As can be seen in Fig. 7, even for stronger pressure steps the bubble returns to an almost spherical shape at later times of the expansion phase again.

An example of the bubble radius vs. time history is shown in Fig. 8. The displayed points were computed as an average from two mutually perpendicular bubble diameters. Due to the bubble shape distortion the experimental points within the expansion phase represent only a rough estimate of an equivalent radius. As was said above this is true for stronger pressure steps primarily. In the case of weaker steps the bubble continues, preserving the spherical shape for even longer times. For a better evaluation of the significant radii R_i, R_{m1}, and R_{M2}, the experimental points in Fig. 8 were fitted by a curve $R(t)$. The initial radii R_i, as determined from different records were very reproducible and it was found that $R_i = 1.65 \pm 0.05$ mm.

4. Results and discussion

Using the experimental arrangement described above, oscillations of nitrogen bubbles in glycerine were studied in great detail under a variety of conditions. By changing the pressure step Δp the amplitude of bubble oscillations, A, could also be varied (see eq. (9)). The bubble wall motion was recorded by a rotating mirror camera and the radiated acoustic waves by a needle hydrophone. From the radius vs.

Fig. 9. Variation of the normalized data with the pressure step Δp^*; (o) experiment, (——) theory.
a) First minimum radius Z_{m1},
b) First damping factor α_1,
c) First compression time T_{zc1},
d) Second oscillation time T_{zo2},
e) First pressure peak in the radiated wave p_{zp1},
f) Second pressure trough in the radiated wave p_{zt2},
g) Acoustic energy in the leading edge of the first bubble pulse $\Delta E'_{za1}$,
h) Acoustic energy in the trailing edge of the first bubble pulse $\Delta E''_{za1}$,
i) Total acoustic energy in the first bubble pulse ΔE_{za1},
j) First bubble pulse effective width ϑ_{z1}.

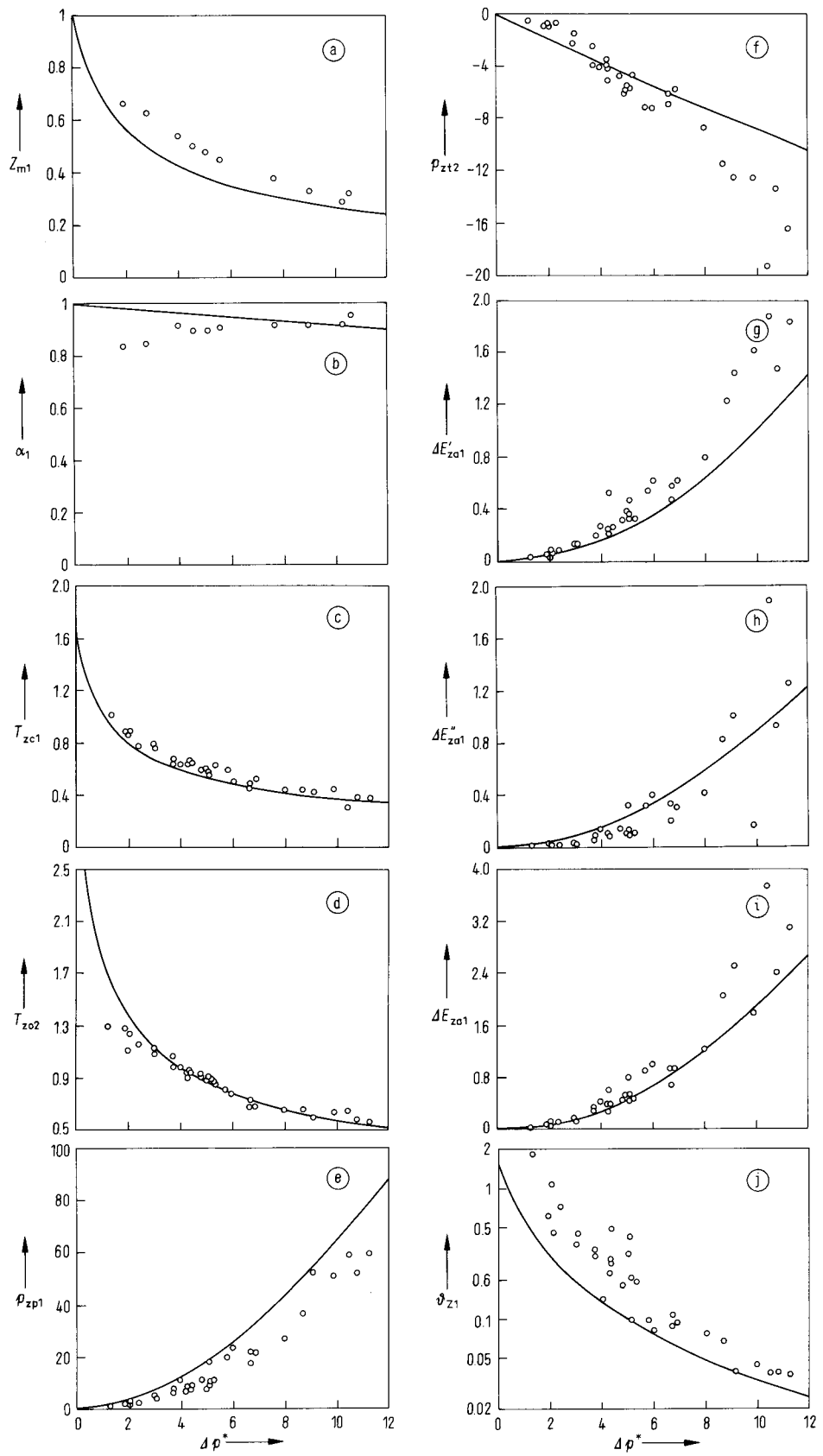
a
b
c
d
e
f
g
h
i
j
Z_{m1}
α_1
T_{zc1}
T_{zo2}
p_{zp1}
p_{zt2}
$\Delta E'_{za1}$
$\Delta E''_{za1}$
ΔE_{za1}
ϑ_{z1}
Δp^*
Δp^*

Fig. 9

time histories (Fig. 8) it was possible to determine the initial bubble radius R_i, the first minimum radius R_{m1}, and the second maximum radius R_{M2}. From the pressure vs. time records (Fig. 5) a number of further quantities could be determined. These are the time of bubble compression, T_{c1}, the time of oscillation, T_{o2}, the peak and trough pressures, p_{p1} and p_{t2}, respectively. Processing the measured waveforms using relations (4) and (5) also yields the acoustic energy in the bubble pulse leading edge, $\Delta E'_{a1}$ (by integrating p_a^2 from 0 to T_{c1}), the acoustic energy in the bubble pulse trailing edge, $\Delta E''_{a1}$ (by integrating p_a^2 from T_{c1} to $T_{c1} + T_{o2}/2$), the total acoustic energy in the bubble pulse, ΔE_{a1} ($\Delta E_{a1} = \Delta E'_{a1} + \Delta E''_{a1}$) and the effective bubble pulse width, ϑ_1 (by integrating p_a^2 from 0 to $T_{c1} + T_{o2}/2$). The same quantities were also computed using the theoretical model (eqs. (1) to (5)). Both the experimental and theoretical data were normalized using the following relations:

$$Z = R/R_i, \quad T_z = T/[R_i(\varrho_\infty/p_{\infty i})^{1/2}],$$

$$p_z = (p/p_{\infty i})\, r/R_i, \quad \Delta p^* = \Delta p/p_{\infty i},$$

$$\Delta E_{za} = \Delta E_a/(\tfrac{4}{3}\pi p_{\infty i} R_i^3), \quad \vartheta_z = \vartheta/[R_i(\varrho_\infty/p_{\infty i})^{1/2}].$$

Variations of the normalized data with the pressure step Δp^* are displayed in Fig. 9.

Comparison of the individual theoretical and experimental time histories $R(t)$ and $p(t)$ (Figs. 2, 3, 5 and 8) shows relatively good agreement. However, a few deviations can be noted, and these deviations can be traced even more distinctly in Fig. 9. First, it can be seen that the differences between the theoretical and experimental values are usually larger for weaker steps Δp^*. Another deviation can be seen in the damping factor α_1 (Fig. 9b), where for stronger steps Δp^*, the experimental values of α_1 are even larger than the theoretical ones (this agrees with the more negative experimental trough pressures p_{zt2} in Fig. 9f). Such a finding is interesting because the larger values of α_1 usually indicate smaller energy losses. However, this does not seem to be the case here (though for bubbles of the size considered, the thermal losses will play a certain role, the theoretical model does not account for them) and an explanation should be sought elsewhere.

In the case of the minimum radii Z_{m1} (Fig. 9a), the experimental values are larger than the theoretical ones. This again corresponds well with the lower values of experimental peak pressures p_{zp1} (Fig. 9e). The reason for the larger Z_{m1} and lower p_{zp1} is evidently the damping of the bubble wall motion which is in fact stronger than was assumed in the theoretical model.

Theoretical and experimental values of T_{zc1} and T_{zo2} (Figs. 9c and 9d) show rather good agreement. However, it can be seen again that the difference between theory and experiment is larger for weaker steps Δp^* than for stronger ones.

From the graphs $\Delta E'_{za1}$ and $\Delta E''_{za1}$ (Figs. 9g and 9k) it follows that in the experiment more acoustic energy is radiated in the leading edge of the bubble pulse than is predicted by the theory. The measured total radiated acoustic energy ΔE_{za1} (Fig. 9i) is also slightly higher. The more intensive acoustic energy radiation during the compression phase (first of all for weaker Δp^* – see also Fig. 9j) results in a less violent compression of real bubbles. This partially explains why the measured times T_{zc1} and radii Z_{m1} are larger than the theoretical values.

Let us now summarize all these findings. Comparison of the theoretical and experimental values in Fig. 9 reveals that even if there is a rather good agreement between theory and experiment there are still certain differences. These differences can partly be attributed to the deformed bubble shape (only a spherical shape is considered by theory at present). Further inaccuracies may be due to omission of the thermal losses in the theoretical model. However, it does not seem that all the differences can be explained in this way. For example, as said above, the deviations are larger for weaker pressure steps Δp^*, but in this case the bubble preserves its spherical shape and the thermal losses should be small. It is also not clear why the bubbles in the experiment radiate acoustic energy in the leading edge of the bubble pulse more intensively than predicted by the theory. Lastly, it is hard to explain at present why the experimental bubbles expand excessively ($\alpha_1 = Z_{M2}$) for stronger steps Δp^*. As mentioned above we do not think that the explanation of this phenomenon should be sought in smaller energy losses.

To obtain a better understanding of the deviations observed new experiments should be performed with more emphasis laid on the controversial points. The theoretical model used for comparison should also be improved by considering the bubble shape deformations, thermal losses and interaction of the bubble with a plane driving pressure step (which, of course, is the cause of the bubble shape deformations).

5. Conclusion

A shock tube proved to be a useful tool for the study of bubble dynamics. Combined observations with a rotating mirror camera and a needle hydrophone made it possible to obtain a rather complete information both on the bubble wall motion and on the radiated acoustic waves. By varying the pressure step Δp it was possible to study the bubbles oscillating with different intensities and under different ambient pres-

sures. In the experiments reported, the ambient pressure p'_∞ ranged from 0.24 to 1.23 MPa and thus the amplitude of oscillations, A_1, ranged from 1.23 to 1.82.

Our initial goal of throwing more light on excessive energy losses has not been reached. In fact, it was found that for the oscillation amplitudes considered agreement between theory and experiment is relatively good. However, some deviations exist. These concern, for example, excessive values of the second maximum radius and minimum pressure, larger values of the first minimum radius and corresponding smaller peak pressures, and a more intensive acoustic radiation during the compression phase. Partial explanations for these phenomena can be found in deformed bubble shapes and neglected thermal losses. But these two mechanisms do not seem to be able to explain all the deviations. Thus further both experimental and theoretical studies are necessary to gain a better understanding of these phenomena.

Acknowledgement

One of the authors, KV, was supported by Heinrich Hertz Stiftung during this research, which is gratefully acknowledged.

References

[1] Blake, J. R., Gibson, D. C., Cavitation bubbles near boundaries. Annu. Rev. Fluid Mech. **19** [1987], 99–123.

[2] Smereka, P., Birnir, B., Banerjee, S., Regular and chaotic bubble oscillations in periodically driven pressure fields. Phys. Fluids **30** [1987], 3342–3350.

[3] Beylich, A. E., Dynamics and thermodynamics of spherical vapour bubbles. VDI Forschungsheft No. 630, 1985, 1–27 (in German).

[4] Samek, L., A multiscale analysis of nonlinear oscillations of gas bubbles in compressible liquids. I. Main resonance. Czech. J. Phys. **B39** [1989], 1354–1365.

[5] Samek, L., A multiscale analysis of nonlinear oscillations of gas bubbles in compressible liquids. II. First and second subharmonics and harmonics. Czech. J. Phys. **B39** [1989], 1366–1371.

[6] Bazhenov, V. Yu., Vasnetsov, M. V., Soskin, M. S., Taranenko, V. B., Dynamics of laser-induced bubble and free-surface oscillations in an absorbing liquid. Appl. Phys. **B49** [1989], 485–489.

[7] Ward, B., Emmony, D. C., Conservation of energy in the oscillations of laser-induced cavitation bubbles. J. Acoust. Soc. Amer. **88** [1990], 434–441.

[8] Vogel, A., Lauterborn, W., Time-resolved particle image velocimetry used in the investigation of cavitation bubble dynamics. Appl. Optics **27** [1988], 1869–1876.

[9] Ward, B., Emmony, D. C., Interferometric studies of the pressures developed in a liquid during infrared-laser-induced cavitation-bubble oscillation. Infrared Phys. **32** [1991], 489–515.

[10] Beylich, A. E., Gülhan, A., On the structure of nonlinear waves in liquids with gas bubbles. Phys. Fluids **A2** [1990], 1412–1428.

[11] Vokurka, K., Amplitudes of free bubble oscillations in liquids. J. Sound Vib. **141** [1990], 259–275.

[12] Smulders, P. T., van Leeuwen, H. J. W., Experimental results on the behaviour of a translating gas bubble in water due to a pressure step. In: Finite-amplitude wave effects in fluids, L. Bjørnø, ed., IPC Science and Technology Press, Guildford 1974, pp. 227–233.

[13] Fujikawa, S., Akamatsu, T., Experimental investigations of cavitation bubble collapse by a water shock tube. Bull. JSME **21** [1978], 223–230.

[14] Gülhan, A., Beylich, A. E., Some investigations about the dynamics of gas bubbles. Acustica **63** [1987], 276–282 (in German).

[15] Vokurka, K., Comparison of Rayleigh's, Herring's, and Gilmore's models of gas bubbles. Acustica **59** [1986], 214–219.

[16] Vokurka, K., The use of a shock tube in bubble dynamics studies. Czech. J. Phys. **B42** [1992], (to appear).